

Fig. 3 Mercury mission using Venus swingby (1973).

For illustrative purposes, the contour chart for the 1986 Mars-Venus opposition from Part 6 is shown in Fig. 1. The chart is in two parts: the left side shows the characteristics of the outbound (Venus swingby) leg and the right side illustrates the direct, return trajectory. The chart graphically illustrates the variation in velocities at Earth and Mars, and in Venus passage distance and date. Parameters relevant to Venus passage appear only on the left side of the chart, since this is an outbound swingby. Note that the region of feasible solutions is constrained by the 1.0 Venus passage distance contour.

Part 7 and Part 8

Direct trajectories to Jupiter, Saturn, Uranus, and Neptune are given in Part 7. Part 8 contains Jupiter swingby missions to Saturn, Uranus, Neptune, or Pluto and also the Outer Planet Grand Tour (a mission which passes Jupiter, Saturn, Uranus, and Neptune). All trajectories with Earth departure velocities less than 0.65 emos and reasonable trip times were included in the tabulation.

An example of a contour chart from Part 8 is shown in Fig. 2, namely, a Saturn mission using Jupiter swingby with launch date in 1977. The relevant speeds and Jupiter passage parameters are shown as contours of constant values. Note that Saturn arrivals before about J.D. 244 4100 are not possible because of the Jupiter passage distance constraint. The dark, nearly vertical line up the center of the chart separates the type one transfers (transfer angles $<180^\circ$) on the Earth-Jupiter leg from the type two transfers ($>180^\circ$).

Part 9

Part 9 contains direct and Venus swingby trajectories to Mercury for the time period 1973 to 1985. A 13-year period was selected to encompass one Earth-Mercury synodic cycle. Characteristics of the direct missions are essentially repeated every 13 years so that trajectories outside this time period can be estimated. There are 3 and occasionally 4 direct launch opportunities to Mercury every year. Only the trajectories associated with the minimum Earth departure velocity launch opportunity of each year are listed in detail in the Handbook. For each of the other launch opportunities, the characteristics of a single trajectory with minimum Earth departure velocity are given.

Launch opportunities for Venus swingby missions to Mercury occur every 19 months. Detailed trajectory information for each launch opportunity from 1973 to 1985 (except 1977 which has extremely high Earth departure velocities) is available. Figure 3 is an example contour chart for the 1973 launch opportunity. It shows the speeds at Earth and Mercury and the parameters relevant to Venus passage: the date, and either periapsis distance, R_p , or Venus encounter

Table 1 SP-35 summary

PART	SUPPLEMENT	DESTINATION PLANET	TRAJECTORY MODE	YEARS
6	A,B,C	σ	♀ SWINGBY	1975-1999
7	A	α	DIRECT	1981-1986 ^a
	A	η	DIRECT	1976-1986
	B	δ	DIRECT	1976-1986
	B	ψ	DIRECT	1976-1986
8	A	η	♂ SWINGBY	1976-1980
	A	δ	♂ SWINGBY	1978-1982
	A	ψ	♂ SWINGBY	1978-1982
	A	π	♂ SWINGBY	1976-1980
	A	ψ	GRAND TOUR	1976-1980
9	-	γ	DIRECT	1973-1985
	-	γ	♀ SWINGBY	1973-1985

^a DATA FOR 1970-1980 ARE CONTAINED IN PART 5 OF THIS HANDBOOK SERIES.

ΔV if R_p is less than 1.05 radii. The encounter ΔV is that ΔV required to perturb the post-encounter trajectory so that the minimum passage distance at Venus can be maintained at 1.05 radii. The trajectories which require an impulsive maneuver at Venus are included in the tabular data if $\Delta V \leq 1000$ m/sec. An additional constraint, imposed on all Mercury handbook data, requires that the Earth departure excess speed be less than 0.60 emos.

It is hoped that Parts 6-9 will be a useful addition to the trajectory handbook series. As new missions become of interest, for example, the modified Grand Tours (Earth, Jupiter, Saturn, Pluto or Earth, Jupiter, Uranus, Neptune), the preparation of new handbooks will be considered.

Reference

- ¹ *Space Flight Handbooks, Vol. 3—Planetary Flight Handbook*, Pts. 1-3, 1963, George C. Marshall Space Flight Center, NASA SP-35.

Selection of Astronaut Cooling Systems for Extravehicular Space Missions

D. C. HOWARD* AND R. G. SYVERSEN†

United Aircraft Corporation, Windsor Locks, Conn.

BECAUSE of man's inherently low efficiency, the metabolic oxidation of food hydrocarbons results in the production of large amounts of thermal energy with very little useful work output. If this excess energy is not removed or transferred to the external environment, it will accrue within the relatively large thermal mass of the crewman's body. Skin temperatures are then elevated by the body's liquid transport system which transfers this heat from the interior. The phenomenon is signified by increasing mean body temperatures and reduced effectiveness of the human machine. If body heat storage is not controlled, physiological tolerance limits will be exceeded.³ The reduced effectiveness is brought about by three major factors: 1) eye irritation, visor fogging, and general discomfort due to massive sweating without evaporation; 2) exhaustion and collapse due to excessive body heat storage; 3) dehydration from prolonged sweating.

Accumulated data on extravehicular activity (EVA), have demonstrated the inadequacy of astronaut gas cooling systems for sustained periods of high work rate. Liquid cooling

Received May 23, 1969; presented as Paper 69-617 at the AIAA 4th Thermophysics Conference, San Francisco, Calif., June 16-18, 1969; revision received February 9, 1970.

* Assistant Project Engineer.

† Analytical Engineer.

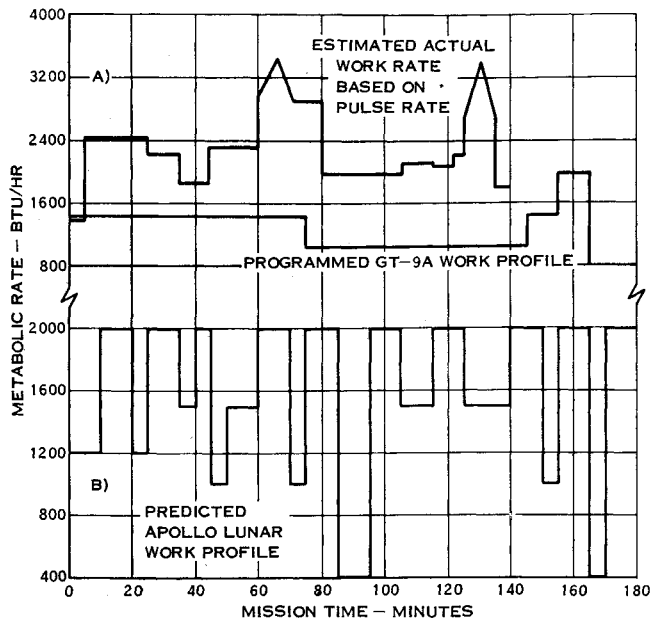


Fig. 1 Apollo mission metabolic profile.

systems, however, are capable of removing the heat generated by higher and more sustained metabolic rates with substantially less physiological stress to the crewman.⁵ What combination, then, of metabolic rate and mission length dictates the selection of liquid over gas cooling?

Mission and Work Rate

Let us start by determining the mission times that must be considered and the peak and average metabolic rates applicable to each. The Gemini Program included EVA excursions of durations of up to 5.5 hr (Gemini XII total EVA¹). Metabolic rates during these activities ranged from resting to more than 3000 Btu/hr. Figure 1a shows that on Gemini 1X-A the actual work rates were greatly in excess of those predicted, resulting in an overload of the cooling system. The crewman experienced high sweat rates, fatigue, and visor fogging. Figure 1b shows that the work rates and mission times predicted for Apollo lunar surface explorations are higher than those predicted for Gemini. Table 1 shows the estimated pressure-suited crewman energy expenditure for typical tasks encountered both on the lunar surface and in free space.² Several of the tasks require work rates substantially higher than the predicted peak rate of 2000 Btu/hr for the Apollo mission. Post-Apollo missions will involve greater metabolic rates and longer stay times.

Thermal Control Requirements

Successive layers of aluminized Mylar separated by spacer materials provide an effective thermal radiation barrier under

Table 1 Metabolic cost of various pressure suit activities

Task description	Ref.	Gravity field	Metabolic cost, Btu/hr
Level walking at 1.5 mph	1	1	2000
Level walking at 2.0 mph	6	1	2350
Ladder climb (9.3 ft in 30 sec)	5	1	1480
Erecting a telescope and platform	5	1	975
Walking up 10% grade at 1 mph	1	$\frac{1}{6}$	600
at 2 mph	1	$\frac{1}{6}$	800
at 5 mph	1	$\frac{1}{6}$	1550
Walking down 10% grade at 5 mph	1	$\frac{1}{6}$	1000
Loping on level at 7 mph	1	$\frac{1}{6}$	2100
Jumping at 9 fps	1	$\frac{1}{6}$	2100

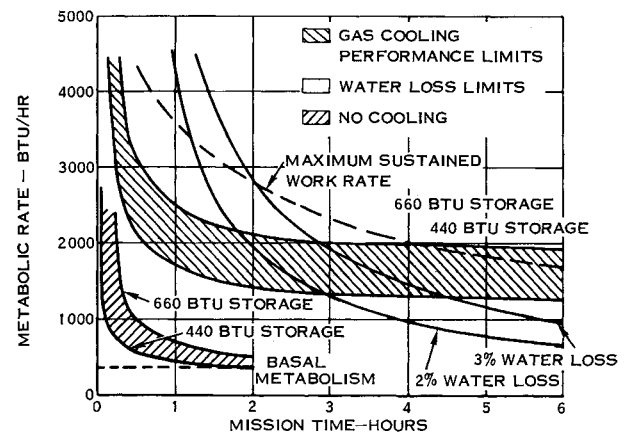


Fig. 2 Water loss limits-gas cooling system for a 165-lb crewman.

space vacuum conditions. A selective optical coating is used on helmet visors to block damaging ultraviolet energy, reflect excessive visible energy (yet provide sufficient visibility under dark conditions), and control infrared energy to the extent required to maintain visor surface temperatures. Passive thermal control techniques, however, are of little use in controlling the fluctuating thermal output of a crewman. An active thermal control system is required to function over a wide range of metabolic rates on demand from the astronaut, independently of light/dark orientation. The two types of systems developed to meet this requirement are the gas-cooled and liquid-cooled systems. Gas cooling relies principally on evaporative heat pickup to achieve thermal control, while liquid cooling depends on conductive heat transfer from the crewman's skin.

As a reference point, we can consider what could be done without cooling. NASA data indicate a range of maximum allowable body heat storage from 440 to 660 Btu.³ Body heat storage and its effect upon mission duration when no cooling system is employed are shown in the lower left corner of Fig. 2. The missions using no cooling system are of such short duration or low metabolic rate that their use is not envisioned for any future practical extravehicular missions.

Gas Cooling Data

Data from manned suit testing performed at Hamilton Standard indicates that heat removal rates for gas cooling systems are limited to approximately 1800 Btu/hr. This value depends on the suit inlet flow conditions and the system chosen (for example, flush flow, fan-battery recirculating, ejector, and so on). Flush flow systems are those which dump all flow overboard. Fan-battery recirculating systems revitalize the atmosphere by CO₂ and H₂O removal with O₂

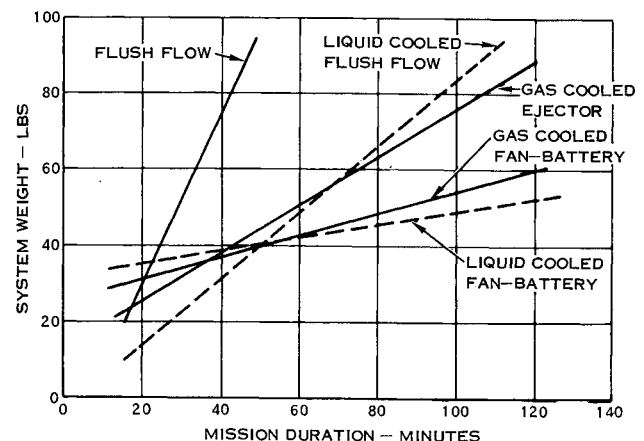


Fig. 3 Gas cooling system weight vs mission duration.

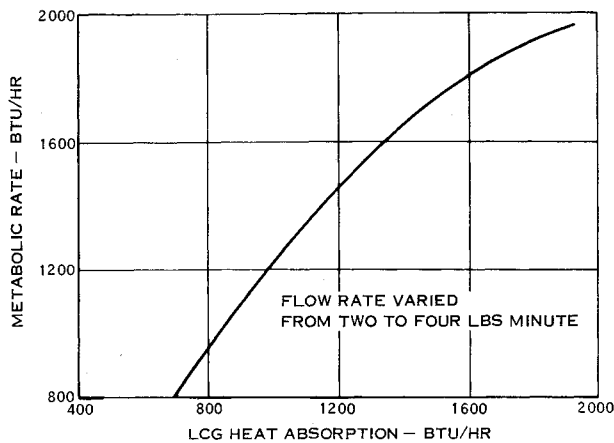


Fig. 4 LCG heat absorption metabolic rate with flow rates of 2 to 4 lb/min.

makeup. Nothing is lost overboard except leakage. Ejector systems dump only that fraction of the gas flow required to maintain acceptable levels of partial pressure O_2 and partial pressure CO_2 . The latent portion accounts for approximately 90% of the total heat removal rate, with sensible heat removal making up the difference. Two gas cooling performance curves are illustrated in Fig. 2 for different allowable body heat storages. The upper performance limit represents a gas-cooled flush-flow system. The gas cooled fan-battery recirculating flow system, because of its higher suit inlet dew-point, has a maximum heat removal rate of 1200 Btu/hr. This system, with an allowable body heat storage of 440 Btu, represents a lower limit of gas cooling system performance. A gas-cooled ejector system performance curve would lie slightly above the lower curve. Figure 2 also illustrates a maximum sustained work rate curve for a healthy man as a function of time.³ It is substantially above the maximum gas cooling system performance curve. Any mission energy expenditures which lie above the gas cooling limits must then be handled by a liquid cooling system, but before discussing liquid cooling systems another limiting factor should be examined.

Additionally, Fig. 2 illustrates the interaction of maximum gas cooling performance with limiting water loss (sweat) conditions. A water loss range of 2 to 3% of body weight is shown as the limiting condition for a typical 165-lb crewman.³ This amount of water loss is generally accepted as resulting in fatigue for most subjects. Therefore, heat removal rates

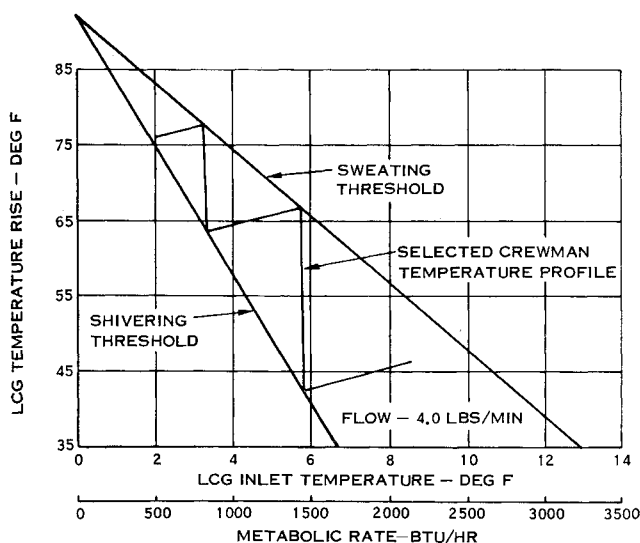


Fig. 5 Subject comfort thresholds vs LCG performance.

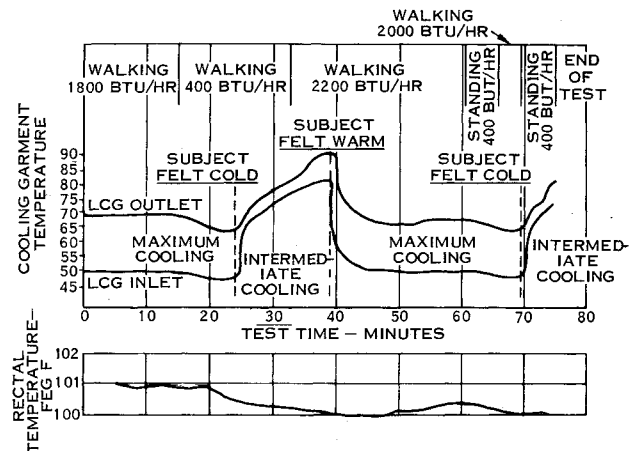


Fig. 6 Liquid cooling system manned test at 4.0 lb/min flow rate.

achieved with gas cooling are adequate for some conditions, but water loss limitations demonstrate the inadequacy of a gas cooling system for missions having Apollo metabolic requirements and durations beyond 2 or 3 hr. This limitation is pointed out again in the description of the Gemini XI mission where the following statement is made: "Although EVA termination may not have been caused by vision impairment from perspiration, the results of this EVA emphasized the limitations of a gaseous-flow cooling system."¹

Even though gas cooling system performance is within water loss limits, there may be reasons why a different system would be selected. The actual selection of a gas cooling system is a parametric consideration (weight, volume, and so on). Thus, an acceptable gas-cooled system may be parametrically inferior to its liquid-cooled counterpart since the weight flows required to achieve maximum thermodynamic performance necessitate larger fans with significantly heavier batteries (or multistage ejectors with higher gas storage quantities to make up that portion of the total flow flushed to space). Moreover, the scheduling of multiple successive missions with inadequate water makeup time available must be considered in the selection of a cooling system. Figure 3 illustrates a typical parametric consideration for three principal types of gas cooling systems as well as for two different liquid cooling systems. The design mission in this case is for a 30-min, 2000 Btu/hr emergency extravehicular transfer.

Liquid Cooling Data

Missions requiring cooling in excess of evaporation of 2 or 3% of body weight must use liquid cooling to preclude intolerable physiological stress. The liquid cooling system referred to hereafter is the Apollo liquid cooling garment (LCG).⁵ It is a loose mesh garment with a series of small flexible tubes sewn in. The tubes are placed so that they are in direct contact with the crewman's skin. Cool water is pumped through the tubes, thereby absorbing the metabolic heat which has been transported to the body's surface by the blood stream.

Let us examine the parameters which size this liquid cooling system. This is best done by referring to data from manned testing performed at Hamilton Standard in support of the Apollo program. First, the system must transfer from the body the amount of heat necessary to prevent excessive sweat loss. Figure 4 shows the results of manned tests conducted in which the liquid flow rate through an LCG was varied during exercise.⁴ The data show heat removal at the same metabolic rate to be largely independent of coolant flow rate. An over-all heat-transfer coefficient of 42 ± 4.6 Btu/hr/°F was calculated for flow rates of 2, 3, and 4 lb/min at a constant coolant inlet temperature of 45°F. However, sweat rate and subject discomfort increased markedly as coolant flow rate

was progressively reduced. This demonstrated that heat removal by itself is insufficient to size the system. A series of tests was run to determine skin temperatures at which active sweating and shivering begin for various metabolic rates.⁵ This testing revealed comfort thresholds illustrated in Fig. 5. The next requirement was to integrate the test results in a concept that could be used to size liquid cooling systems. This was accomplished by designing a system in which the inlet temperature could be varied without changing flow rate. This method of varying LCG inlet temperature is accomplished by a valve which directs all or a portion of the fluid from the LCG to a heat exchanger whose output is mixed with the uncooled fluid and supplied back to the LCG. The selected three-step temperature profile that is within comfort thresholds is shown in Fig. 5 for a fixed flow of 4 lb/min.

Figure 6 illustrates a portion of a manned test conducted at Hamilton Standard utilizing an optimized liquid cooling system. Treadmill speed has varied for a calibrated test subject to determine the ability of the system to maintain crewman comfort when the metabolic rate was step-changed from 1800 to 400 Btu/hr and back to 2200 Btu/hr. Coolant flow was maintained at 4 lb/min and the subject was free to select his cooling garment inlet temperature by manually setting one of three diverter valve positions. Subject comments were noted and liquid temperatures continually monitored throughout the test duration. A point to be noted is the lag of human physiology compared to the response of the mechanical system. Despite these lags, a no-sweat condition was maintained. Figure 5 illustrates the maximum heat removal rate that can be achieved with this liquid cooling system (with a water flow of 4.0 lb/min) while maintaining the subject below the sweating threshold. Although current liquid cooling systems have not demonstrated heat removal rates greatly in excess of 2000 Btu/hr, development of tubing with thinner walls, materials with increased conductivity, and different tubing configurations is expected to result in achievement of heat removal rates in excess of 3000 Btu/hr. Further performance gains are hampered by the body's limitation in transferring heat from the interior to the skin surface. Additionally, as shown in Fig. 2, sustained crewman work rates in excess of 3000 Btu/hr for more than an hour and a half are probably not attainable.

References

- ¹ Summary of Gemini Extravehicular Activity, NASA SP-149, 1967, pp. 4-55.
- ² Summary of Man's Physical Capabilities on the Moon, CR-66119, Vol. III, NASA.
- ³ Bioastronautics Data Book, SP-3006, Feb. 9, 1967, NASA.
- ⁴ Hamilton Standard Engineering Report, SVHSER 4250, 1967, Windsor Locks, Conn.
- ⁵ Jennings, D., "Water-Cooled Space Suit," *Journal of Spacecraft and Rockets*, Vol. 3, No. 8, Aug. 1966, pp. 1251-1256.

Attitude Controllability of a Satellite with Flywheels

H. I. WEBER* AND W. SCHIEHLEN†
Technical University of Munich, Germany

FLYWHEEL attitude control systems require the desaturation of angular momentum accumulated by non-cyclic external torques. This can be done by control thrust

Received September 16, 1969; revision received September 16, 1969.

* Instructor, COPPE (University of Rio de Janeiro) with Fellowship at Institute B of Mechanics.

† Chief Engineer, Institute B of Mechanics.

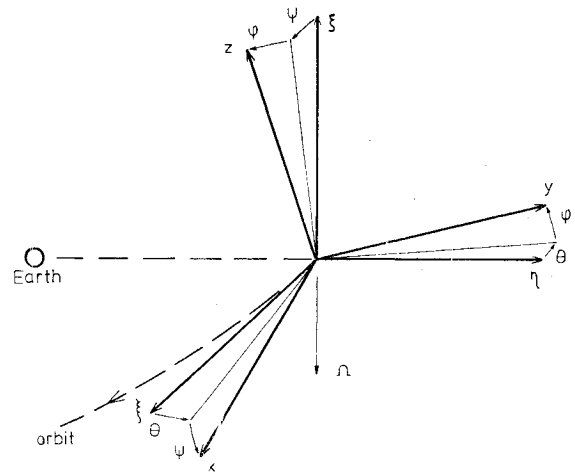


Fig. 1 Reference frame.

jets or, as recently shown by Frik,¹ using the gravity gradient phenomenon. Usually the control phase and the desaturation phase change periodically. But the satellite control and the flywheel desaturation can be done simultaneously, too. For this purpose, the state vector of the satellite is extended by adding the angular velocity of the flywheels. So both will be controlled, the satellite to the desired position and the wheel velocity to zero, using an external desaturating torque. A convenient way to prove this simultaneous desaturation is with the controllability concept.

Take a satellite containing three flywheels in a circular earth orbit to be positioned in the local vertical, characterized by a reference frame ξ, η, ζ , Fig. 1. The deviations of the satellite from the reference frame are described by pitch angle θ , roll angle ϕ , yaw angle ψ . The flywheel axes are assumed parallel to the satellite principal axes x, y, z . Due to control, angles θ, ϕ, ψ are small all the time.

Euler Equations

$$A_x \dot{\omega}_x + J_x \dot{\nu}_x + (A_x \omega_x + J_x \nu_x) \omega_y - (A_y \omega_y + J_y \nu_y) \omega_z = M_x \quad (1)$$

(x, y, z cyclic perm.)

and the motion equation of the flywheels

$$J_x (\dot{\omega}_x + \dot{\nu}_x) = u_x \quad (x, y, z \text{ cyclic perm.}) \quad (2)$$

build up our system. A and ω are the satellite principal moments of inertia and angular velocities, respectively, J and ν the same for the flywheels, u the control moment.

It will be proved first that when external torque $M \equiv 0$, the satellite can't be desaturated, i.e., the system isn't controllable. This is the problem of a orbiting vertical-positioned gyrost at without external forces. We introduce the state vector $x = \{\omega_x \omega_y \omega_z \nu_x \nu_y \nu_z\}^T$, where $\omega_z' = \omega_z + \Omega$ (Ω orbiting velocity), and linearize (1) and (2) about zero equilibrium position.

So we obtain

$$\dot{x} = Ax + Bu \quad (3)$$

$$A = \begin{bmatrix} 0 & a_2 & 0 & 0 & -a_4 & 0 \\ -a_1 & 0 & 0 & a_3 & 0 & 0 \\ 0 & 0 & 0 & 0 & 0 & 0 \\ 0 & -a_2 & 0 & 0 & a_4 & 0 \\ a_1 & 0 & 0 & -a_3 & 0 & 0 \\ 0 & 0 & 0 & 0 & 0 & 0 \end{bmatrix} \quad B = \begin{bmatrix} -b_{1x} & 0 & 0 \\ 0 & -b_{1y} & 0 \\ 0 & 0 & -b_{1z} \\ b_{2x} & 0 & 0 \\ 0 & b_{2y} & 0 \\ 0 & 0 & b_{2z} \end{bmatrix}$$

where

$$a_1 = [(A_z - A_x)/(A_y - J_y)]\Omega$$